Hydrogen bond cooperativity in simulated water: Time dependence analysis of pair interactions

F. Sciortino and S. L. Fornili[a)]
Physics Department, University of Palermo, Via Archirafi 36, I-90123 Palermo, Italy

(Received 31 August 1988; accepted 1 November 1988)

Hydrogen bonding in water systems is investigated by introducing a new method to analyze the time dependence of pair-interaction data obtained from a molecular dynamics simulation of 216 ST2 [F. H. Stillinger and A. Rahman, J. Chem. Phys. **60**, 1545 (1974)] water molecules at 280 K. This approach avoids the use of cutoff values and yields a more realistic bond population, whose distributions of geometric and energetic properties are reported as a function of the bond lifetimes. For the fraction of long-lived bonds, correlation among bond stability, molecular mobility, and local structure is elecited. Percolation analysis of HB network evidences cooperativity in the spatial distribution of bonds, which does not originate from proton polarizability of HB and/or from many-body terms of the interaction potentials since a rigid water model and pair potentials are used. These features can play a role in the anomalous properties of liquid water.

I. INTRODUCTION

The anamolous properties exhibited by liquid water are the macroscopic expression of microscopic cooperative mechanisms.[2] Interestingly, computer simulations using additive pairwise water–water potentials reproduce many of these properties,[1,3,4] suggesting that cooperative behavior can originate from mechanisms which do not involve proton polarizability of hydrogen bond (HB)[5] and/or many-body terms of interaction potentials.[6,7]

Several papers have been published on geometric and energetic properties of HBs, and on the extent and structure of hydrogen bonding in aqueous systems. In particular, percolation analysis[8–11] applied to computer simulation data has shown that liquid water at room temperature can be envisioned as a self-structuring macroscopic space-filling network of bent and strained HBs.[8,9] Further, many authors have analyzed simulated water, in search of self-stabilizing and/or self-replicating HB structures. Four-bonded molecules,[12] unstrained polyhedral species[2] and pentagonal rings[13,14] are some of such structures. Also, geometric,[3] statistical,[12] and stereodynamic[15,16] factors have been proposed to account for the abovementioned polarization-independent cooperativity.

In the present work we investigate HB lifetimes and topological characteristics of networks formed by the more stable fraction of bonds among ST2 water molecules simulated at 280 K, with the aim of enlighting connections between HB lifetimes and HB structures at molecular and supramolecular levels (i.e., in local environment and in network organization) in liquid water simulated using pairwise potentials.

The paper is organized as follows: in Sec. II we briefly discuss problems that arise if time-dependent properties of HBs are studied with commonly used HB definitions. Further, a new method to analyze HB lifetimes is introduced. Results obtained using this method are reported in Sec. III; in Sec. III A the dependence of some relevant geometric and energetic quantities upon HB lifetimes is discussed; in Sec. III B we evidence a relationship among bond stability, local structure and water mobility; and in Sec. III C topological properties are evaluated for the network formed by the fraction of the stabler bonds.

II. THE METHOD

The two most common definitions of HB (sometimes compounded together) are: (i) Energetic: Two water molecules are considered to be H-bonded if their interaction energy is lower than a given value V_{HB}. The dimer interaction energy function has a smooth shape[2] which prevents a unique choice of V_{HB}. This problem is normally obviated using a range of V_{HB} values. (ii) Geometric: Two molecules are considered bonded if the values of pertinent internal coordinates of the dimer are within appropriate ranges. For water dimer, such coordinates are the oxygen–oxygen distance R_{OO}, the hydrogen–oxygen–oxygen angle θ_H, the lone pair (LP)–oxygen–oxygen angle θ_{LP}, and the dihedral angle δ between the planes H–O–O and LP–O–O.[10,17] To define these coordinates, the atom (or pseudoatom) participating in the bond is taken as the hydrogen atom (or lone pair) on the donor water closest to the oxygen atom of the acceptor water.[10] In the ST2 water model the lone pair pseudoatoms coincide with the negative charges.

These definitions are only partially suitable to study dynamic properties of H bonding. Indeed, water molecules show a librational motion on a time scale of 10^{-13} s superimposed to slower diffusional and rotational motions, which causes a time variation of dimer interaction parameters. Therefore, the lifetimes of bonds with parameters oscillating not too far from the HB definitions limits, can appear much shorter than they really are, if a definition of HB based on cutoff values is used.[18–20]

To obviate this distortion, we decided to perform the present bond time dependence analysis considering all the attractive pair interactions (API) between molecules whose R_{OO} distance is smaller than 3.5 Å, with no further restriction. The 3.5 Å value is roughly the first-minimum position

[a)] C.N.R.-I.A.I.F., Via Archirafi 36, I-90123 Palermo, Italy.

 0021-9606/89/052786-07$02.10

of the O–O pair correlation function of water, which is slightly greater than the HB distance (3.4 Å) suggested by x-ray and neutron diffraction experiments.[21] Thus, the API set of a given configuration includes all HBs present in that configuration as well as some non-HB interactions. This is, of course, an exceedingly permissive condition. Nevertheless, realistic HB distribution functions, not affected by the artifact mentioned above, are readily obtained from a bond lifetime analysis based on API sets, as we shall see in the following.

The data analyzed in this work were obtained from a 20 ps molecular dynamics (MD) simulation at 280 K of 216 ST2 particles confined to a cubic box of 18.6 Å side length. Periodic boundary conditions were used to simulate the condensed phase. The system density was 1 g/cm^3 and the integration timestep was 0.002 ps. Snapshots were recorded on every five timesteps. From these data, 80 system configurations (called C configurations in what follows) spaced by 0.2 ps were chosen, whose API sets were used as initial data to select links with lifetimes longer than given τ values, according to a logical AND procedure. Two molecules are considered linked by a bond lasting more than τ ps, if their interaction energy is negative and their R_{OO} distance is less than 3.5 Å in *all* the snapshots occurring in a τ ps long time interval centered on the selected C configuration. In particular, the $\tau = 0$ case corresponds to the usual hybrid energetic–geometric HB definition[8] with $V_{HB} = 0$. A link breakage followed by reformation within the time interval between consecutive snapshots is undetectable. On the other hand, we expect few events of this kind since the time interval between successive snapshots is in our case 0.01 ps long (i.e., 5×0.002 ps), that is at least one order of magnitude smaller than typical water relaxation times.[22]

Time-dependent properties of molecular bonding in the simulated system can be investigated by analyzing API sets corresponding to different τ values. Indeed, increasing the τ values, bonds with shorter lifetime are progressively filtered off.

III. RESULTS AND DISCUSSION

A. Energetic and geometric distributions

In this section we discuss the energetic and geometric properties of the API set as a function of bond lifetime. In Fig. 1(A) we show the pair interaction energy distributions

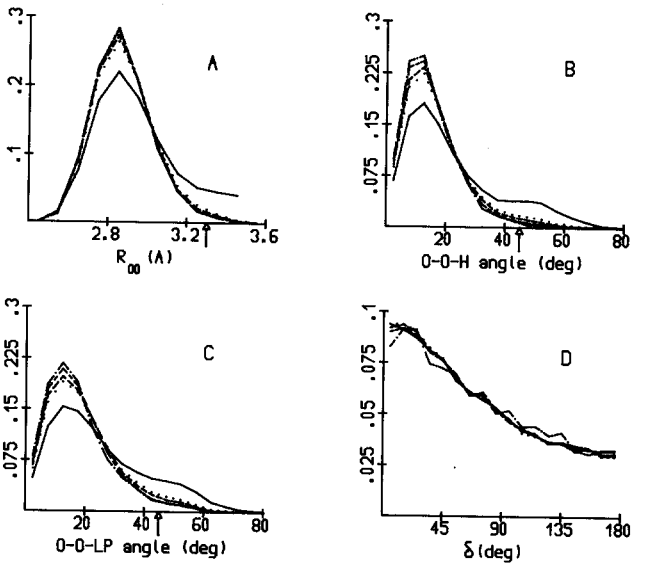

FIG. 2. Normalized distribution functions of the API set for the internal coordinates of water dimer. The same τ values and symbols are used as in Fig. 1. (A) oxygen–oxygen distance R_{OO}; (B) oxygen–oxygen–hydrogen angle Θ_H; (C) oxygen–oxygen–lone pair angle Θ_{LP}; (D) dihedral angle between the planes H–O–O and LP–O–O, δ. The arrows indicate commonly used values for strong geometric hydrogen bond definitions (Ref. 10).

for links whose lifetimes exceed some selected τ values (0, 0.35, 0.75, 2.25, and 3.95 ps). In Fig. 1(B), the same curves are reported after normalization of the underlying areas (each of which expresses the population of bonds surviving for a time longer than the corresponding τ value). In Fig. 2 we show, the normalized distributions for the internal coordinates R_{OO}, θ_H, θ_{LP}, and δ, using the same symbols as in Fig. 1. The arrows in Figs. 1 and 2 indicate values commonly assumed to define strong "geometric"[10] or "energetic" HB. The mean and rms values for these energetic and geometric distributions are collected in Table I together with the total number of analyzed links and the average number of bonds per molecule with lifetime longer than τ ps.

The following comments are in order: (i) for τ values larger than ~ 0.4 ps, the above distributions are slightly affected by the specific choice of τ. (ii) The geometric distributions satisfy very well the criteria proposed for the geometric definition of strong HB (Fig. 2), while the agreement

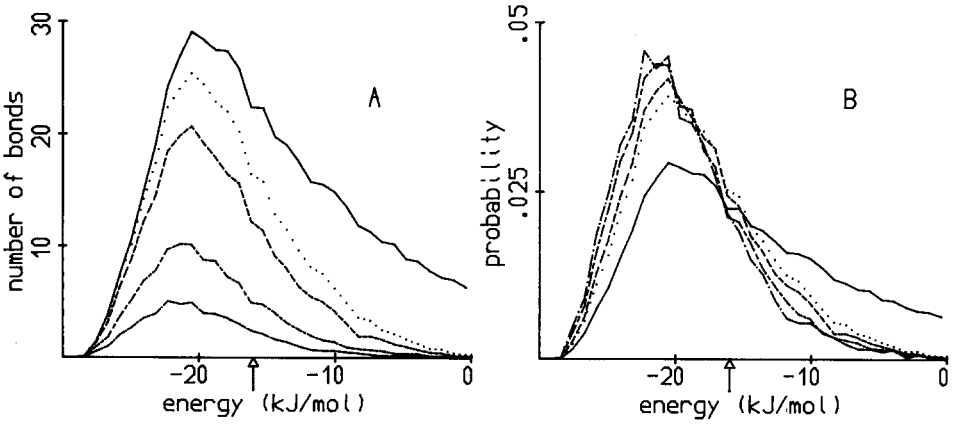

FIG. 1. (A) Pair interaction distribution function of the API set (see the text) for some τ values: full line $\tau = 0$; dotted line $\tau = 0.35$; dashed $\tau = 0.75$; double dashed $\tau = 2.25$; dash–dotted $\tau = 3.95$ ps). (B) Same curves normalized to unitary area. The arrow indicates the most commonly used value for a strong energetic hydrogen bond definition (Ref. 1).

TABLE I. Total number of analyzed bonds N, mean number of bonds per molecule n_{HB} with lifetimes longer than τ ps, and mean and rms values for the distributions reported in Figs. 1 and 2. Units are ps, Å, degree, and kJ/mol.

τ	N	n_{HB}	$\langle R_{OO}\rangle$	$\sigma_{R_{OO}}$	$\langle\theta_H\rangle$	$\sigma_{\theta H}$	$\langle\theta_{LP}\rangle$	$\sigma_{\theta LP}$	$\langle E\rangle$	σ_E
0.00	39 716	4.6	2.94	0.21	22.5	15.9	24.9	15.8	− 15.4	6.5
0.05	35 877	4.1	2.91	0.18	20.7	14.6	23.3	14.9	− 16.4	5.8
0.35	25 976	3.0	2.88	0.16	17.2	11.5	20.1	12.6	− 18.0	4.9
0.75	19 879	2.3	2.87	0.15	16.3	10.5	19.1	11.8	− 18.5	4.7
1.05	16 771	1.9	2.87	0.15	15.9	10.1	18.7	11.5	− 18.8	4.7
1.45	13 589	1.6	2.87	0.15	15.6	9.8	18.4	11.2	− 19.0	4.6
1.85	11 172	1.3	2.87	0.15	15.4	9.6	18.2	11.1	− 19.1	4.6
2.25	9 279	1.1	2.87	0.15	15.3	9.4	18.0	11.0	− 19.2	4.5
3.05	6 508	0.7	2.87	0.15	15.1	9.3	17.8	11.0	− 19.4	4.5
3.95	4 406	0.5	2.87	0.15	14.8	9.1	17.5	10.9	− 19.6	4.5

between energetic distributions and the energetic definition of strong HB (Fig. 1) is within 70%. In the latter case the chosen V_{HB} value (− 16 kJ/mol) corresponds to an approximate temperature-invariant point in the ST2 pair potential distribution.[1] (iii) The average number of bonds per molecule calculated using geometric as well as energetic definitions of *strong* HB ($n_{HB} = 2.2$)[1] compares very well with the average number of bonds per molecule surviving more than 0.75 ps ($n_{HB} = 2.3$), as reported in Table I. These observations suggest that API links having a lifetime longer than ~0.4 ps can be considered as HBs. For shorter times the API set contain also some non-HB interactions which are characterized by larger R_{OO} values and/or higher interaction energy (see Figs. 1 and 2 and Table I). (iv) No significant change in δ is observed as a function of τ, suggesting that this internal coordinate is not relevant to the HB description, as already pointed out.[10]

Since, as shown in Figs. 1 and 2 and Table I for $\tau > 0.4$ ps, energetic and geometric distributions of bonds depend slightly on bond lifetimes, energetic or geometric parameters alone *do not* provide a characterization of the water dimer adequate to investigate the HB time dependence. This suggests than an ampler set of molecular parameters is needed.

The API set analysis as a function of τ provides the possibility of selecting the statistically most relevant HB structures and to evaluate their properties without diversion by the abovementioned artificial bond breakages connected with HB definitions based on cut-off values.

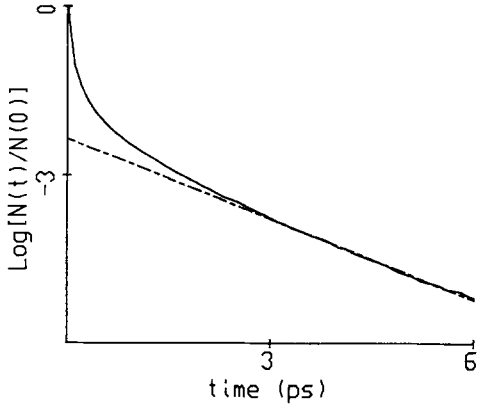

FIG. 3. Normalized decay function $N(t)$ of the API bonds (full line); long-time tail best-fitting straight line (with 2.0 ps slope) (dashed line).

To characterize the time dependent properties of the stable fraction of API links, we introduced a decay function $N(t)$ which is defined as the number of links still present after a time t since their first appearance.[19] This function has been calculated by using an API set involving all system configurations stored during the MD simulation. In Fig. 3 we show on a logarithmic scale the normalized $N(t)$ function vs time. The decay is clearly nonexponential, in agreement with previously reported results.[18,19] For times greater than ~3 ps, however, the $N(t)$ plot can be fitted by a straight line with 2.0 ps slope.

According to the above observations on the time analysis of the energetic and geometric properties of the API set, we interpret the intial part of this curve as the decay of non-HB interactions, an the part corresponding to times longer than 0.4 ps as HB decay. The single-exponential tail of $N(t)$ can be assigned to the most stable HBs. The 2.0 ps value is in the range of the results obtained analyzing simulations data according to energetic definitions of HB[18,19] and it agrees with experimental findings.[23]

B. Properties of stably and unstably linked molecules

Aiming to characterize the influence of bond stability on structural and dynamic properties of ST2 water molecules, we have selected two groups of molecules with 20 particles each. The first group (stable group) includes the 20 molecules with the longest-lived bonds during the present 20 ps MD simulation; the second group (unstable group) includes 20 molecules whose bonds do not last longer than 4 ps. Quadratic mean displacement, $\langle[\mathbf{r}(t) - \mathbf{r}(0)]^2\rangle$, and running coordination number $n(r)$—that is, the average number of neighbors which are found within a sphere of radius r, $n(r) = 4\pi\rho\int g(r)\cdot r^2\,dr$, ρ being the number density and $g(r)$ the radial distribution function—have been evaluated for these two groups as well as for the whole system. In these calculations all recorded MD data have been used. Results are shown in Fig. 4 for the quadratic mean displacements and in Fig. 5 for the running coordination numbers, where the full lines refer to the stable group, the dashed lines to the unstable group, and the dotted lines to the whole system. In Fig. 6 we report the difference $\delta n(r)$ between the coordination numbers of the unstable and stable groups:

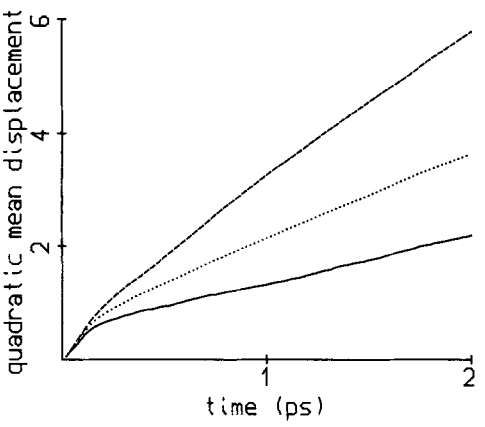

FIG. 4. Quadratic mean displacement (in Å^2), $\langle[\mathbf{r}(t)-\mathbf{r}(0)]^2\rangle$, of molecules with long-living bonds (full line), of the whole system (dotted line), and of unstably linked molecules (dashed line). Data averaged over the 20 ps extension of the MD simulation.

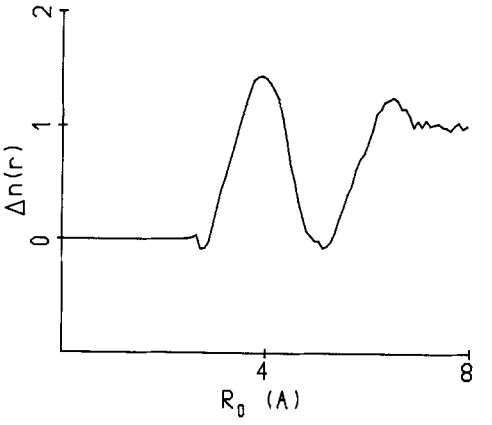

FIG. 6. Differences in local density, as measured by $\delta n(r) = n(r)_{\text{unst}} - n(r)_{\text{st}}$, between groups of molecules with unstable and stable bonds.

$$\delta n(r) = n(r)_{\text{unst}} - n(r)_{\text{st}}.$$

Self-diffusion coefficients evaluated from the long-time slope of the quadratic mean displacements are 0.7, 2.05, and 1.2×10^{-5} cm^2/s for the stable group, the unstable group and the whole system, respectively. The latter value coincides with a previously reported result relative to MD simulation of ST2 water at the same temperature.[19] The corresponding experimental value is 1.5×10^{-5} cm^2/s.[24] The diffusion coefficients relative to the unstable (stable) group mimic a temperature increase (decrease) of ~10 K with respect to the average temperature of the present simulation. However, due to the small number of particles of the simulated system and to the arbitrary group composition, these equivalent temperature variations should only be considered as indicative of a rather large multiplicity of states and properties of liquid water. The difference in self-diffusion between stable and unstable groups suggests an increase of structure around most stably linked molecules.[25] This is confirmed by the data reported in Fig. 5, which show that indeed the structural order is different for the two groups. The number of the nearest neighbors within a 3.3 Å distance are 4.7 and 5.4 for the stable and unstable groups, respectively. Further, a lower local density is associated with the stable group, as measured by the limiting value of $\delta n(r)$ shown in Fig. 6. This result parallels previous findings obtained analyzing the difference of the so-called "patches" of four-bonded and non-four-bonded water molecules.[19] Results shown in Fig. 6 indicate that the above mentioned lower density regions extend to ~7 Å, in agreement with previous findings.[19] It is worth noting that in Ref. 19 a hybrid energetic–geometric HB definition was used.

To summarize, molecules with more persisting bonds are characterized by lower mobility, lower local density, and enhanced structure, confirming the relevant interplay between geometry and dynamics in liquid water.[16] Further, since fluctuations in local density and local entropy of liquid water are related to its anomalous thermodynamic properties,[12] the present results suggest a connection between HB lifetime and anomalous properties of liquid water. Analogous correlations among mobility and local order have been previously evidenced analyzing MD water simulations at various densities and constant temperature.[26]

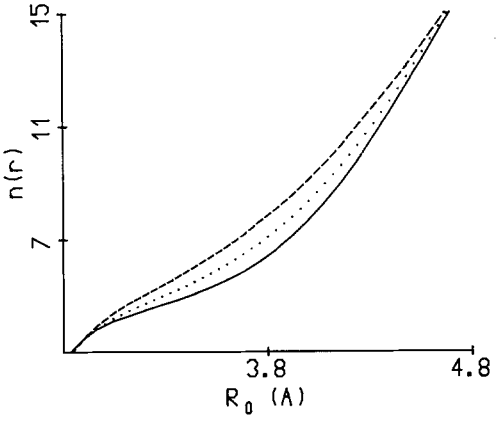

FIG. 5. Running coordination number $n(r)$ as a function of the oxygen–oxygen distance r for molecules with long-living bonds (full line), for the whole system (dotted line), and for unstably linked molecules (dashed line). Data averaged over 20 ps.

C. Analysis of bond network connectivity

In the framework of bond percolation analysis, the connectivity properties of the systems are analyzed as a function of the probability p_b that two adjacent sites are bonded. Varying p_b from 0 to 1, the system undergoes a transiton from a small-cluster phase to a completely connected phase. At a critical value of the bonding probability p_c an infinite cluster appears which spans the whole system.[27]

Topological properties of HB networks in simulated liquid water have been investigated associating p_b to the average number of HB per molecule n_{HB} via the relationship $p_b = n_{\text{HB}}/4$, and varying n_{HB} through different choices of V_{HB}.[8,9] A good agreement between ST2 data and random bond percolation theory has been found, speaking for the absence of a correlation in the spatial distribution of bonds.[8,9] Small but systematic deviations between theoretical random bond distributions and computer simulation data for ST2 water, which become larger as the temperature is decreased,[19] have been interpreted as the effect of a weak

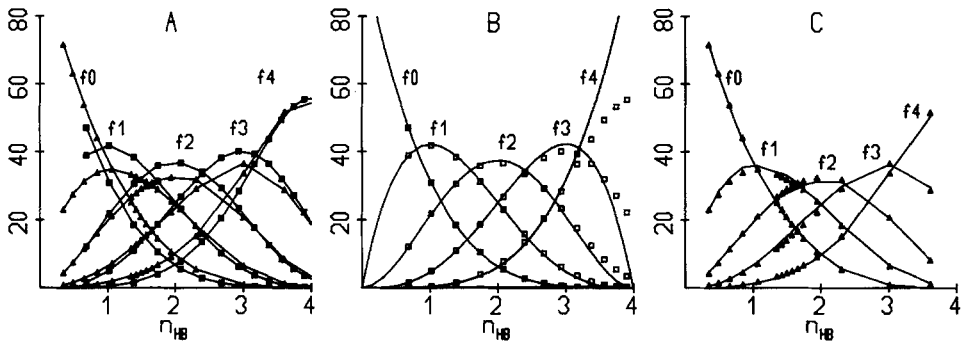

FIG. 7. (A) Fractions f_j of water molecules having j intact bonds ($j = 0$–4) evaluated using energetic bond definition (EC) (□) or bond time-stability criterion (TC) (△). In this part of the figure full lines are only drawn as eye guides. (B) f_j for EC data (□) compared with the binomial distribution of Eq. (1) (full line) using $p = n_{HB}/4$ and $z = 4$. (C) f_j for TC data (△) compared with the results of the Monte Carlo fitting procedures of Eq. (2) (full line).

correlation among connected sites.[19] This effect adds to the well known geometrical cooperativity among connected sites.[9]

As suggested by the discussion of Sec. III, the presence of correlation in the spatial bond distribution can be masked by energetic HB definitions. Aiming to evidence such a correlation, we have investigated the connectivity properties of the HB network as a function of the bond lifetime, following the time evolution of the API set, whose connectivity has been analyzed according to procedures described in Refs. 8 and 9.

A second connectivity analysis has been performed on the API set, where n_{HB} was varied by selecting energy thresholds V_{HB}, rather than bond lifetimes τ. The results of this energetic analysis, which are reported for comparison in the following figures, coincide with previously published findings.[8,9] Therefore, differences in connectivity properties of HB networks resulting from application to the API set of the above procedures—time-stability analysis and energetic analysis—cannot be attributed to different spatial positions of molecules (i.e., to different pseudolattice) or to different statistical features.

In Fig. 7 we report results concerning the fractions f_j of molecules that are linked to j neighbors vs n_{HB}. For a random distribution of bonds we have,[9]

$$f_j = \binom{z}{j} p_b^j \cdot (1 - p_b)^{z-j}, \tag{1}$$

where z is the coordination number of the network and $p_b = n_{HB}/z$.

In Fig. 7(A) we show the f_j functions evaluated using the above time-stability criterion (TC) (△) and energetic criterion (EC) (□) analyses. For all n_{HB} values, f_0 and f_4 values are larger for TC than for EC data, indicating that (i) the same total number of bonds is distributed over a lower number of molecules in the TC case as compared with the EC case and (ii) that the probability of four-bonded sites is higher in the TC case than in the EC case. Therefore, a higher connectivity is apparent in the HB network if the time-stability criterion is used to define n_{HB}. In Fig. 7(B), EC data are reported with superimposed (full line) random bond theoretical f_j values obtained from Eq. (1), with $z = 4$. Since the EC f_j values agree with the theoretical predictions, any difference between EC and TC data must be ascribed to correlation among bonds. These results clearly show that the bond network of simulated ST2 water does not appear, at least at the presently simulated temperature, as a random bond network, if the connectivity is probed varying n_{HB} according to the above outlined time-stability criterion.

To further investigate this correlation effect, we have fitted the TC f_j data according to some bond distribution rules, using the following Monte Carlo procedure:

(a) Randomly pick up a bond within the API set corresponding to $\tau = 0.05$ ps. This τ value has been chosen rather than $\tau = 0$, to take away the fastest decaying bonds.

(b) Evaluate the bond breakage probability p_l according to the chosen rule.

(c) Compare this p_l with a random number p_r evaluated with a uniform random number generator.

(d) Delete the selected bond if p_l is greater than p_r.

(e) Repeat from (a) until all the links are deleted.

In Fig. 7(C) we report TC data (△) together with the results (full line) obtained using this procedure with the following bond-breakage rule, which provides the best agreement with TC data:

$$p_l = \begin{cases} 1 & \text{if at least one of the two molecules linked by the randomly chosen band has more than four bonds} \\ 1 - 0.09 \times k & \text{if the randomly chosen bond connects molecules with up to four bonds; } k \text{ is the total number of bonds of the two linked molecules} \end{cases} \tag{2}$$

As mentioned above, a number of bond-breakage rules have been tried, some of them favoring the stability of four-bonded molecules. However, the best agreement with TC data was yielded by Eq. (2).

These findings confirm that (i) there is a correlation in bond distribution, which favors a spatial bond condensation, and (ii) that the bond lifetime is strongly coupled to the complete environment of the linked molecules, in agreement

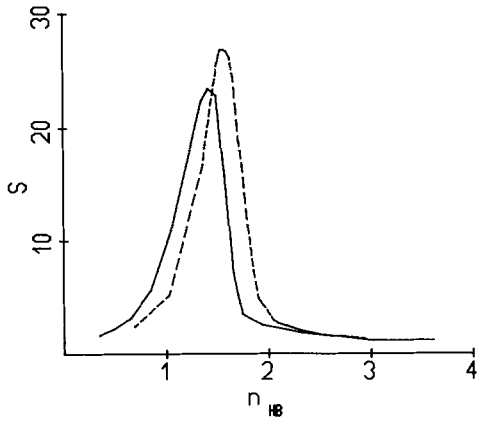

FIG. 8. Mean cluster size S evaluated according to the energetic (dashed line) and time-stability (full line) criteria.

with the results discussed in Sec. III. (iii) Further, Eq. (2) suggests that the bond lifetime probability does not favor a specific coordination number, being proportional to the total number of bonds, i.e., to the local connectivity of the sites. (*iv*) The longest-living bonds are those which connect four-bonded molecules. This agrees with the results concerning the running coordination number $n(r)$ and self-diffusion coefficient of the stably bonded group of molecules, that have been discussed in Sec. IV.

The presence of a spatial bond condensation is also confirmed by the data reported in Figs. 8 and 9, where plots are shown of the mean cluster size S and of the fraction of molecules belonging to the infinite cluster p_∞, respectively, vs n_{HB}, which have been evaluated according to both TC (full line) and EC (dashed line) criteria. Indeed, the position of the maximum of S (Fig. 8) identifies a critical value p_c which is lower for TC than for EC data, suggesting that in TC data a smaller number of bond per molecule is sufficient to form an infinite cluster. Since the same lattice is used in both cases, the higher percolation efficiency must be ascribed to bond correlation effects. The same effect on the

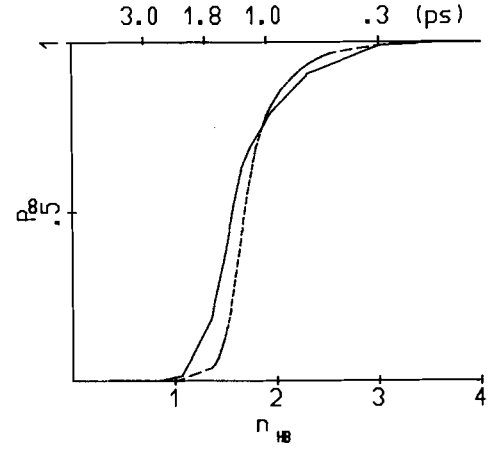

FIG. 9. Fraction of molecules belonging to the infinite cluster p_∞ according to energetic (dashed line) and time-stability (full line) criteria. The nonlinear upper scale has been constructed using τ and n_{HB} data reported in Table I.

critical p value is found, if S and p_∞ are evaluated for the case of four-bonded water molecules as in Ref. 19.

When the time stability is used as a criterion to vary n_{HB}, p can be interpreted as a decay function of the percolative properties of the HB network, and a percolative persistence time can be associated to the critical value p_c. As one can see from Fig. 9, the cluster of the API set retain percolative properties up to ~ 1.5 ps at 280 K, and liquid water would appear as a macroscopic gel, if observed for shorter times. The equivalent persistence time for the percolation of four-bonded sites is ~ 0.2 ps, suggesting that at the presently simulated temperature, non-HB interactions provide strong contributions to the percolative characteristics of four-bonded molecules. These two percolation persistence times could be assumed as useful parameters to analyze the liquid water properties in the metastable region of the temperature–density place.

IV. CONCLUSIONS

In this work we have studied the properties of the attractive pair interactions (API) among adjacent molecules in ST2 water as a function of bond lifetimes at a simulated temperature of 280 K. This approach provides a new method to calculate energetic and geometric distributions of hydrogen bonds, which does not imply any choice of cutoff values. A particularly relevant result of this analysis is that the HB lifetime is not directly determined by its energetic value only.

Some dynamic and structural properties have been evaluated for molecules with long-living bonds, which have been compared with the corresponding properties of unstably bonded molecules as well as with the average properties of the whole system. Self-diffusion coefficient and running coordination number for stably and unstably linked molecules have been calculated. Differences in these properties show a correlation among bond stability, molecular mobility, and enhanced local order. These differences persist for the two groups of molecules at least up to 20 ps (i.e., the time extension of the present MD simulation). Further, stably linked molecules are characterized by low local density. This feature has been previously observed for four-bonded patches of ST2 water[9] and in the environment of a MCY water molecule with restricted mobility.[28]

Results of bond network connectivity analysis as a function of bond lifetimes are also presented. These data are interpreted in terms of correlated bond distribution and compared with results of a MC fitting procedure that indicates a proportionality between bond stability and local connectivity. Correlation determines an easier cluster formation and a lower percolation threshold as compared with the random bond theory results.[8,9] In particular, the findings of our MC-fitting procedure suggest that the longest-living bonds are those which connect four-bonded molecules.

Weak correlation in bond distribution and tendency of clustering among connected sites were previously suggested on the basis of small but systematic differences between theoretical random bond results and simulation data.[8,19] Such effect is evidenced by the present bond time-stability analysis which enables one to sort out a statistically relevant bond population without incurring problems connected

with the use of cutoff values to define HB.

Cooperativity in liquid water hydrogen bonding is evidenced by the present analysis, although rigid pairwise additive potentials are used to model the water–water interaction. Therefore, since cooperative effects arising from HB polarizability[5] or from many-body contributions[29] are excluded, a HB stabilizing mechanism appears to be present which depends on the water–water interaction geometry.[3,15,16] Further, due to the nonrandom bond distribution, the spatial correlation among four-bonded molecules increases beyond the pure geometrical effect.[9] This introduces in the percolative model of water[12,30] a long-range correlation that would make it consistent with the stability limit conjecture.[13,31] Spatial correlations of HBs in liquid water have been experimentally observed.[32]

The overall picture of liquid water emerging from this study is that of a percolating network of *spatially* correlated hydrogen bonds. The backbone of this network, which is composed of sites with long-living bonds, lower local density and lower mobility, retains percolative characteristics up to ~ 1.5 ps at 280 K.

The application of the presently developed method to analyze MD simulations performed at lower temperature and concentrations could yield useful information on both structural and dynamic properties of water in its metastable region, as well as of the longer-living molecular aggregates.

ACKNOWLEDGMENTS

We wish to thank Professor M. U. Palma, Professor M. B. Palma Vittorelli, Professor L. Cordone, Professor A. Cupane, Dr. M. Migliore, and Dr. V. Martorana for useful discussions, and Professor A. Geiger for the MD and percolation analysis programs. We also thank Mr. G. La Gattuta and Mr. M. Lapis for skillful technical assistance. The present work has been carried out at IAIF-CNR and supported also by local MPI-60% and CRRNSM funds.

[1]F. H. Stillinger and A. Rahman, J. Chem. Phys. **60**, 1545 (1974).
[2]F. H. Stillinger, Science **209**, 451 (1980).
[3]Y. Kataoka, H. Hamada, S. Nosé, and T. Yamaoto, J. Chem. Phys. **77**, 5699 (1982).
[4]O. Matsuoka, E. Clementi, and M. Yoshimine, J. Chem. Phys. **64**, 1351 (1976).
[5]G. Zundel, in *The Hydrogen Bond: Recent Developments in Theory and Experimental Results*, edited by P. Schuster, G. Zundel, and C. Sandorfy (North-Holland, Amsterdam, 1976), Vol. 2.
[6](a) E. Clementi, J. Phys. Chem. **89**, 4426 (1985); (b) J. Detrich, J. Corongiu, and E. Clementi, Chem. Phys. Lett. **112**, 426 (1984).
[7]J. L. Finney and J. M. Goodfellow, in *Structure and Dynamics: Nucleic Acids and Proteins*, edited by E. Clementi and R. M. Sarma (Adenine, New York, 1983), p. 81.
[8]A. Geiger, F. H. Stillinger, and A. Rahman, J. Chem. Phys. **70**, 4185 (1979).
[9]R. L. Blumberger, H. E. Stanley, A. Geiger, and P. Mausbach, J. Chem. Phys. **80**, 5230 (1984).
[10]M. Mezei and D. L. Beveridge, J. Chem. Phys. **74**, 622 (1981).
[11]M. Mezei, Mol. Phys. **52**, 1 (1984).
[12]H. E. Stanley and J. Teixeira, J. Chem. Phys. **73**, 3404 (1980).
[13]R. J. Speedy, J. Phys. Chem. **88**, 3364 (1984).
[14]A. C. Bealch and S. A. Rice, J. Chem. Phys. **86**, 5676 (1987).
[15]S. L. Fornili, M. Leone, F. Madonia, M. Migliore, M. B. Palma-Vittorelli, M. U. Palma, and P. L. San Biagio, J. Biomol. Str. Dyn. **1**, 473 (1983).
[16]M. B. Palma-Vittorelli and M. U. Palma, in *Structure and Motion: Nucleic Acids and Proteins*, edited by E. Clementi, G. Corongiu, M. H. Sarma, and R. H. Sarma (Adenine, New York, 1985).
[17]M. G. Sceat and S. A. Rice, J. Chem. Phys. **72**, 3237 (1980).
[18]D. C. Rapaport, Mol. Phys. **50**, 1151 (1983).
[19]A. Geiger, P. Mausbach, J. Schnitker, R. L. Blumberger, and H. E. Stanley, J. Phys. (Paris) **45**, C7-13 (1984).
[20]D. A. Zichi and P. J. Rossky, J. Chem. Phys. **84**, 2814 (1986).
[21]I. Olovsonn and P. J. Jonsonn, in *The Hydrogen Bond*, edited by P. Schuster, G. Zundel, and C. Sandorfy (North-Holland, Amsterdam, 1976).
[22]D. Eisenberg and W. Kautzmann, *The Structure and Properties of Water* (Oxford University, New York, 1969).
[23]W. Danninger and G. Zundel, J. Chem. Phys. **74**, 2769 (1981).
[24]H. R. Pruppacher, J. Chem. Phys. **56**, 101 (1972).
[25](a) H. G. Hertz, Ber. Bunsenges. Phys. Chem. **3/4**, 183 (1971); (b) **74**, 666 (1970).
[26]A. Geiger, P. Mausbach, and J. Schnitker, in *Water and Aqueous Solutions*, edited by G. W. Neilson and J. E. Enderby (Hilger, Bristol, 1986).
[27]D. Stauffer, *Introduction to Percolation Theory* (Taylor and Francis, London, 1985).
[28]R. Noto, M. Migliore, F. Sciortino, and S. L. Fornili, Mol. Simul. **1**, 225 (1988).
[29]D. Hankins, J. W. Moskovitz, and F. H. Stillinger, J. Chem. Phys. **59**, 995 (1973).
[30]H. E. Stanley, J. Phys. A **12**, 1329 (1979).
[31]R. J. Speedy, J. Phys. Chem. **86**, 982 (1982).
[32]J. L. Green, A. R. Lacey, and M. G. Sceats, J. Phys. Chem. **90**, 3958 (1986).